Received: 13 February 2025 | Revised: 1 April 2025 | Accepted: 12 April 2025

DOI: 10.1002/pen.27235

RESEARCH ARTICLE

POLYMER ENGINEERING AND SCIENCE WILEY

The conditioning relative humidity influences the gas permeability of active films and nanocomposites based on gelatin

Larissa Tessaro[1] | **Paula Benoso**[1] | **Valentina Siracusa**[2] | **Rodrigo Vinícius Lourenço**[1] | **Marco Dalla Rosa**[3] | **Paulo José do Amaral Sobral**[1,4]

[1]Department of Food Engineering, Faculty of Animal Science and Food Engineering, University of São Paulo, Pirassununga, Brazil

[2]Department of Chemical Science (DSC), University of Catania, Catania, Italy

[3]Department of Agricultural and Food Science, University of Bologna, Cesena, Italy

[4]Food Research Center (FoRC), University of São Paulo, São Paulo, Brazil

Correspondence
Larissa Tessaro, Department of Food Engineering, Faculty of Animal Science and Food Engineering, University of São Paulo, Av Duque de Caxias Norte, 225, 13635-900 Pirassununga, SP, Brazil.
Email: larissa.tessaro@usp.br

Funding information
Fundação de Amparo à Pesquisa do Estado de São Paulo; Conselho Nacional de Desenvolvimento Científico e Tecnológico; Coordenação de Aperfeiçoamento de Pessoal de Nível Superior

Abstract

The influence of relative humidity on O_2 and CO_2 permeability of gelatin-based films and nanocomposites incorporated with crystalline nanocellulose (CN), non-encapsulated "Pitanga" (*Eugenia uniflora* L.) leaf extract (PLE) or encapsulated in a water-in-oil-in-water double emulsion (DE) was studied. Cross-section morphology by scanning electron microscopy, crystallinity, moisture content, thickness, and O_2 and CO_2 transmission rate (GTR) were determined. The addition of CN, PLE, and/or DE caused changes in the morphology and crystallinity of the films and nanocomposites. In general, the GTR in films and nanocomposites increased with increasing relative humidity due to the swelling effects and plasticizing effect of water. Nanocomposites with non-encapsulated PLE or DE showed good oxygen barrier properties at high relative humidity. The outcome of this study was that the addition of CN with PLE or DE improved the gas barrier properties of gelatin-based films, especially in high relative humidity conditions.

Highlights

- "Pitanga" leaf extract (PLE) was encapsulated in a double emulsion (DE).
- Crystalline nanocelluloses (CN) were extracted from soybean straw.
- Gelatin nanocomposite films were produced with CN and activated by PLE or DE.
- Relative humidity (RH) influences the O_2 and CO_2 permeability in the films.
- The nanocomposite film with CN/DE showed low permeability to gases at high RH.

KEYWORDS

barrier properties, biopolymer, double emulsion, encapsulation, nanocellulose, Pitanga extract

1 | INTRODUCTION

Gelatin is a well-known protein obtained by partial hydrolysis of collagen from the skin, bones, and connective tissues of animals and produced worldwide. In recent decades, gelatin has been widely studied for the development of biopolymeric films for food packaging applications due to its excellent film-forming capacity, biodegradability, biocompatibility, safety, and because it comes from renewable and natural sources.[1,2] Gelatin-based films are edible, thin, flexible, and semi-crystalline materials with good physical properties but very sensitive to water.[2,3]

Gelatin has a structure formed by polypeptide α-chains (single chain), β (two α-chains joined by covalent bonds), and γ (three α-chains joined by covalent bonds).[4] Additionally, it has a typical Ala-Gly-Pro-Arg-Gy-Glu-4Hyp-Gly-Pro amino acid composition and elemental composition of 50.5% carbon, 25.2% oxygen, 17% nitrogen, and 6% hydrogen.[4] The gelatin structure gives its films great versatility, from the ability to incorporate different types of active components and fillers to the possibility of forming blends with other biopolymers, such as chitosan.[5–7] The addition of other components to gelatin-based films for use as food packaging is intended to improve some of their properties, such as mechanical and/or barrier performances.[8]

The function of a biopolymeric food packaging is to protect the packaged food in a safe and sustainable way, functioning as a barrier to gases and humidity, microorganisms, aromatic compounds, and grease.[9] Specifically, gas permeability is extremely important as it controls the exchange of oxygen (O_2) and carbon dioxide (CO_2) between the inside and outside of the packaging, which directly affects the quality of the packaged food.[10] For example, controlling O_2 permeability is crucial to extending the shelf life of unsaturated lipid-rich foods and foods susceptible to microbial growth, among others, as O_2 induces oxidation reactions and provides a favorable environment for the growth of aerobic microorganisms.[11] On the other hand, it must be sufficient to ensure the respiration of fruits and vegetables and inhibit the growth of anaerobic microorganisms.[10]

Despite their great versatility, gelatin-based films present low performance in terms of mechanical properties, high sensitivity to water, and good gas barrier properties only in conditions of low relative humidity,[1] which limits their application in certain food niches. One of the approaches explored to overcome these disadvantages is to incorporate reinforcing fillers (such as natural fibers or nanoparticulate, as nanocelluloses) in the biopolymeric matrix, forming composite or nanocomposite films.[8,9] Nanocelluloses are nanosized natural fibers extracted from renewable lignocellulosic materials and can satisfactorily act as reinforcing fillers due to their physical properties.[1,12,13]

When nanocellulose is extracted by acid hydrolysis, it can be obtained in the form of crystalline nanocellulose (CN), with a rigid structure due to high crystallinity (>65%), diameters ranging from 2 to 100 nm, and a length of 500 nm to 2 μm.[9,12] As fillers, they can act as a physical barrier to gas, as they are similar in size to the pores created in the biopolymeric network and, therefore, create a tortuous path.[14] CN can also act by improving the mechanical and water sensitivity of gelatin-based packaging.[1,9,13]

On the other hand, the incorporation of active compounds into gelatin-based films for use as food packaging aims to enhance the functionality of these materials, creating the so-called active films.[15] For example, the incorporation of plant extracts, rich in polyphenols, into gelatin-based films can confer antioxidant and antimicrobial activity to these materials.[7,16]

"Pitanga" (*Eugenia uniflora* L.) leaf extract (PLE) is extracted from the leaves of the Pitanga tree (*Eugenia uniflora* L.), a fruit tree found in tropical regions of the world and which has been satisfactorily used to produce active films based on gelatin and other biopolymers with excellent bioactivities.[15,16] The bioactivity of PLE is related to the high polyphenol content in its composition.[17]

PLE can be incorporated into the biopolymeric matrix in free form, which means, as it is[16] or encapsulated into double emulsions.[13,18] Encapsulation can protect the biological properties of active compounds, but encapsulation systems can also improve active packaging properties, such as barrier and mechanical properties.[6] These improvements are cost-effective and can occur due to the interactions between the components of the encapsulated system with the biopolymeric matrix. Moreover, it can contribute to reducing the hydrophilicity characteristic of films due, for example, to the oil emulsion formulation.[11,18]

In this study, gelatin-based active films and nanocomposites were produced with the incorporation of CN extracted from soybean straw by acid hydrolysis and by the addition of non-encapsulated PLE or PLE encapsulated into water-in-oil-in-water double emulsions (DE). To the best of our knowledge, there are no studies on the combined effect of the addition of double emulsions encapsulating plant extracts and CN on the gas barrier properties of films based on gelatin or any other biopolymer. We hypothesize that chemical interactions occurring between gelatin and CN, PLE, and/or DE (hydrogen and ionic bonds, for example) can produce materials that have a lower transmission rate to O_2 and CO_2 under

different relative humidity conditions. The aim of this study was, therefore, to investigate the gas transmission rate in these films and nanocomposites, conditioned at different relative humidity.

2 | MATERIALS AND METHODS

2.1 | Material

Type-B bovine gelatin (molecular weight: ~50 kDa; 250 bloom), sodium caseinate, and Grinsted PGPR® (Polyglycerol Polyricinoleate) were donated by Gelco (Pedreira-SP, Brazil), Alibra Ingredientes SA (Campinas-SP, Brazil), and DuPont (São Paulo-SP, Brazil), respectively. Food grade soybean oil, sodium hypochlorite, and Tween 80 were purchased from Cargill (Primavera do Leste-MT, Brazil), Candura (Piracicaba-SP, Brazil) and Sigma-Aldrich (St Louis, MO), respectively. Acetone P.A., ethanol P.A., sulfuric acid (H_2SO_4) P.A., sodium hydroxide (NaOH) P.A., magnesium sulfate heptahydrate ($Mg_2SO_4{\cdot}7H_2O$), sodium carbonate (Na_2CO_3), hydrogen peroxide (H_2O_2, >50%), and glycerol (≥99.5%) were purchased from Labsynth® (São Paulo-SP, Brazil). Soybean straw was supplied by the Embrapa Soja (Londrina-PR, Brazil).

2.2 | Production of "Pitanga" leaf extract

"Pitanga" (*Eugenia uniflora* L.) leaves were collected at the Faculty of Animal Science and Food Engineering, Pirassununga-SP, Brazil (21°59′46″S, 47°25′36″W). "Pitanga" leaf extract (PLE) was produced using a hot solvent extraction (60% v/v hydroethanolic solvent at 80°C) assisted by ultrasound.[17] The extract obtained was freeze-dried (Freeze-dryer, FD 1.0-60E, Heto-Holten A/S, Allerod, Dinamarca) to produce the PLE. The PLE was stored in the dark at −18°C.

2.3 | Production of double emulsion

The DE was prepared in two steps.[18] In the first step, a single emulsion (SE) was produced using the PLE resuspended in distilled water (1 g PLE freeze-dried/10 mL distilled water) as the inner aqueous phase (20 g/100 g SE) and soybean oil with PGPR (3 g/100 g oil) as the oil phase (80 g/100 g SE). In the second step, DE was produced using the SE as the inner lipid phase (40 g/100 g DE) and distilled water with Tween 80 (3 g/100 g distilled water) and sodium caseinate (0.5 g/100 g distilled water) as the dispersant aqueous phase (60 g/100 g DE). The SE and DE were stored in the dark at 4°C. The properties (droplet size, droplet size distribution, physical stability, morphology, and biological activities, among others) of these emulsions have been studied.[19,20]

2.4 | Production of crystalline nanocellulose

The CN was extracted from soybean straw using alkaline pre-treatment, bleaching, acid hydrolysis, and mechanical treatment.[12] The CN suspension was freeze-dried, and the CN was stored at room temperature. This nanomaterial has been characterized previously.[13]

2.5 | Production of gelatin-based films and nanocomposites

For both films and nanocomposites, the film-forming solution (FFS) was prepared by the hydration of gelatin (4 g/100 g FFS) in distilled water for 30 min, and subsequent solubilization at 55°C for 10 min (Thermostatic bath, MA-184/20, Marconi, Piracicaba-SP, Brazil) and addition of the glycerol (25 g/100 g gelatin). In the case of nanocomposites, the gelatin hydration was carried out in distilled water with CN (4.5 g/100 g gelatin). The DE was added dropwise under a magnetic stirrer integrated with temperature digital control at 500 rpm to FFSs at the concentration of 0.25 g PLE/100 g gelatin.[13,18] Negative and positive-control films and nanocomposites were also made, without the addition of DE or by adding non-encapsulated PLE instead of DE, at the same concentration (0.25 g PLE/100 g gelatin), respectively. The FFSs were transferred to acrylic plates and dried at 30°C for 24 h (forced-air circulation drying oven, MA035, Marconi, Piracicaba-SP, Brazil). Then, six treatments were produced: gelatin-based films without DE (F-C), with DE (F-DE) or PLE (F-PLE) and gelatin-based nanocomposites without DE (N-C), with DE (N-DE) or PLE (N-PLE).

Before analyses, films and nanocomposites were conditioned for 7 days in desiccators at different relative humidity (RH, 0, 34, 59, and 76%) at 25°C. For X-ray diffraction analysis and scanning electron microscopy characterizations, films and nanocomposites were previously conditioned for 15 days in desiccators over silica gel. The main physical and functional properties of these gelatin-based films and nanocomposites (water vapor permeability, solubility in water, UV/Vis light barrier properties, color and opacity, microstructure, thermal properties, mechanical properties and antioxidant activity, among others) were previously characterized, and these data were published by Tessaro et al.[13,18]

2.6 | Films and nanocomposites characterizations

2.6.1 | Scanning electron microscopy

Cryo-fractured cross-section of the films and nanocomposites were analyzed by scanning electron microscopy (SEM, TM3000, Hitachi Ltd., Tokyo, Japan) in a random position at an accelerating voltage of 15 kV.[13] Sample films and nanocomposites were cryo-fractured after quench freezing using liquid nitrogen.

2.6.2 | X-ray diffraction

The X-ray spectrum of films and nanocomposites was obtained using an X-ray diffractometer (Miniflex 600, Rigaku Corporation, Tokyo, Japan) operated at 25°C, 40 kV, and 15 mA (CuKβ radiation, $\lambda = 0.15405$ nm), for a range of angles of $2\theta = 2–70°$ with 2°/min of speed scan.[13] Relative crystallinity was calculated as the ratio between the upper area of the diffraction peak and the total diffraction area.

2.6.3 | Moisture content

The moisture content of films and nanocomposites conditioned at different relative humidity (RH) was determined gravimetrically.[21] Films and nanocomposites samples were dried using a forced-air circulation drying oven at 105°C for 24 h, and the moisture content was expressed as g water/100 g of wet film or nanocomposite.

2.6.4 | Thickness

The thickness of films and nanocomposites was determined using a Sample Thickness Tester DM-G with a digital dial indicator (MarCartor 1086 type, Mahr GmbH, Esslingen, Germany) with associated DM-G software.[22] The reading was made twice per second, with a resolution of 0.001 mm. The minimum, maximum, and average of each reading were recorded in triplicates, in 15 different positions of each film, at room temperature and reported as the mean thickness value, expressed in microns (μm).

2.6.5 | CO_2 and O_2 transmission rate

The gas transmission rate measurement of films and nanocomposites was performed using a manometric method with a Permeance Testing Device, type GDP-C (Brugger Feinmechanik, GmbH, München, Germany), according to ASTM 1434-82 (Standard test Method for Determining Gas Permeability Characteristics of Plastic Film and Sheeting), DIN 53536 in compliance with ISO/DIS 15105-1 and according to the Gas Permeability Testing Manual (Registergericht München HRB 77020, Brugger Feinmechanik GmbH).

As previously described by Siracusa et al.,[22] the equipment consists of two chambers between which the sample (12 × 12 cm) is placed. The chamber on the top of the film is filled with the gas used in the test (CO_2 or O_2), at a pressure of 1 atm. A pressure transducer, set in the chamber below the film, records the increase of gas pressure (P) as a function of time (t). From pressure/time data, the software automatically calculates the permeation rate, which can be converted into permeability knowing the film thickness. The gas transmission rate values (GTR) of the films and nanocomposites were determined considering the increase in pressure in relation to time and the volume of the device.[23] The operating conditions were a temperature of 20°C, a gas stream of 100 cm^3/min, a sample area of 78.4 cm^2, and different RH. Permeability measurements were performed in triplicate, at least.

2.7 | Statistical analysis

The material characterizations were performed with at least three measurements (triplicate) and presented as mean ± standard deviation (SD). Statistical analysis was carried out using Statistica data analysis software system (version 7, StatSoft Inc., GmbH, Hamburg, Germany). Results were analyzed using one-way and two-way analysis of variance (ANOVA) and Tukey's test comparison ($\alpha = 0.05$) for determining significant differences between the means.

3 | RESULTS AND DISCUSSION

3.1 | Scanning electron microscopy

The SEM images showed that the internal structures of the films and nanocomposites were affected by the addition of PLE, CN, and DE (Figure 1). F-C and F-PLE presented more homogeneous, smooth, and compact internal structures compared to the other treatments. This indicated that PLE was satisfactorily incorporated into F-PLE, as observed for gelatin-based films with PLE at higher concentrations.[24]

It was possible to observe white spots and some pores possibly generated by agglomeration of CN particles in

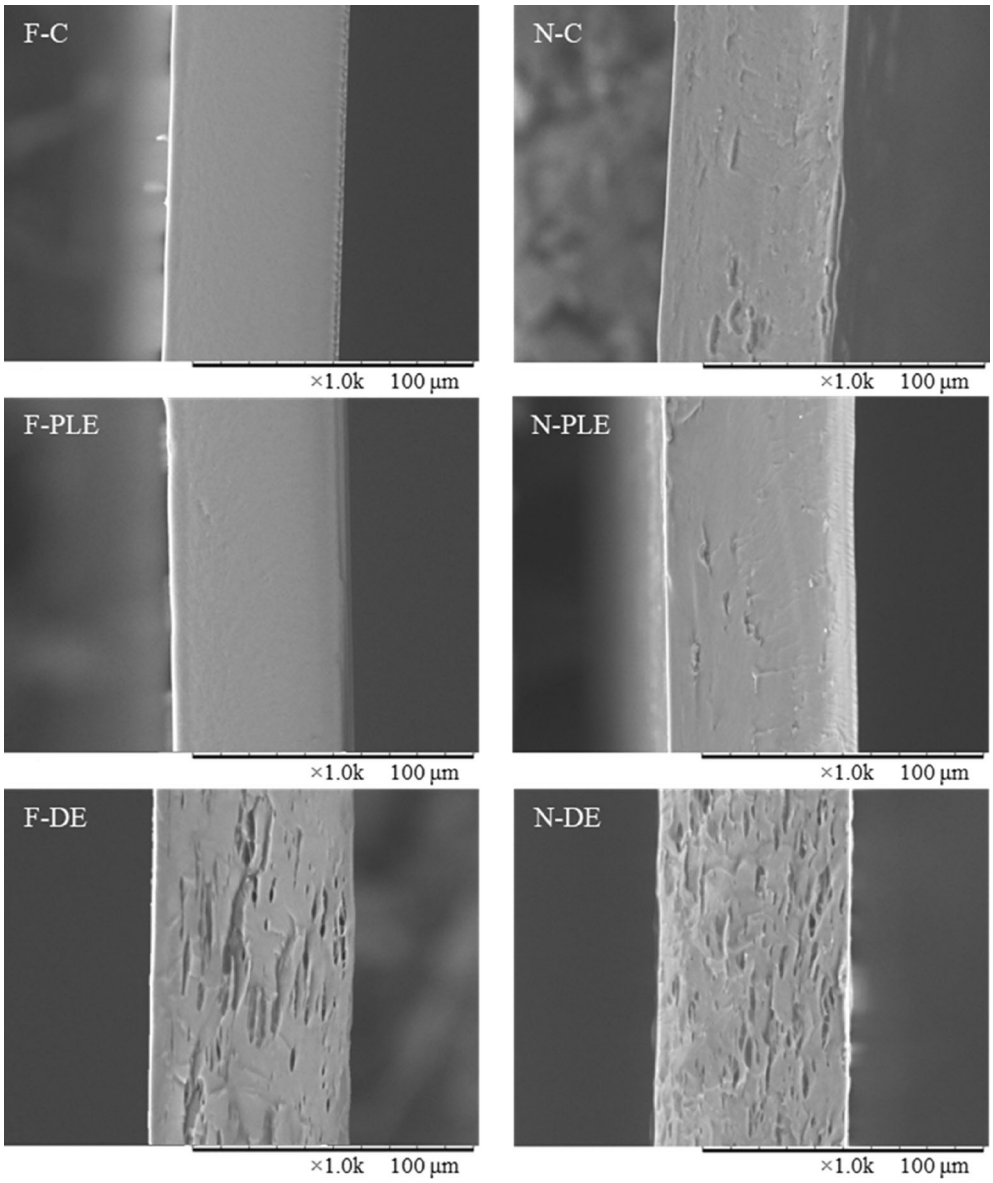

FIGURE 1 Scanning electron microscopy images of the cross-section of gelatin-based films (F) and nanocomposite films (N) control (C), with "Pitanga" leaf extract (PLE), or with double emulsion (DE). The scale bar is 100 µm.

nanocomposites without DE (N-C and N-PLE). In the case of N-PLE, the pores were less visible, which indicates that in the presence of PLE, the CN is better incorporated into the nanocomposite matrix. This may occur due to the complex formed between gelatin and PLE polyphenols, which can help to disperse CN more evenly, reducing agglomerations and increasing homogeneity, as CN can interact with both gelatin and PLE.[5] Vargas-Torrico et al.[25] also observed that pomegranate peel extract agglomerated into films based on gelatin and carboxymethyl cellulose, forming layers, possibly because of the concentration and composition of the extract.

The addition of DE, into both F-DE and N-DE, caused the formation of pores in the internal structure of these treatments, probably due to the presence of DE oil droplets. Despite the changes observed in the internal structure of the different treatments, all incorporated components were well dispersed in the matrix, without causing fractures nor discontinuity.[26] The gelatin matrix surrounded the DE and stabilized the interfaces of different phases, resulting in an internal structure of the film and nanocomposite with homogeneously distributed oil droplets. The emulsifiers present in the external aqueous phase of DE (sodium caseinate and Tween 80) may also have contributed to the uniform dispersion of DE in the film and nanocomposite.[26] Acharya et al.[5] also observed similar morphology on gelatin/bacterial nanocelluloses films with O/W nanoemulsions.

3.2 | X-ray diffraction

The peaks observed at $2\theta = 7.3–9.7°$, and 20–22.8° were characteristic of the α-helix (crystalline) and β-sheet (amorphous) structures of gelatin (Figure 2), respectively.[5,16]

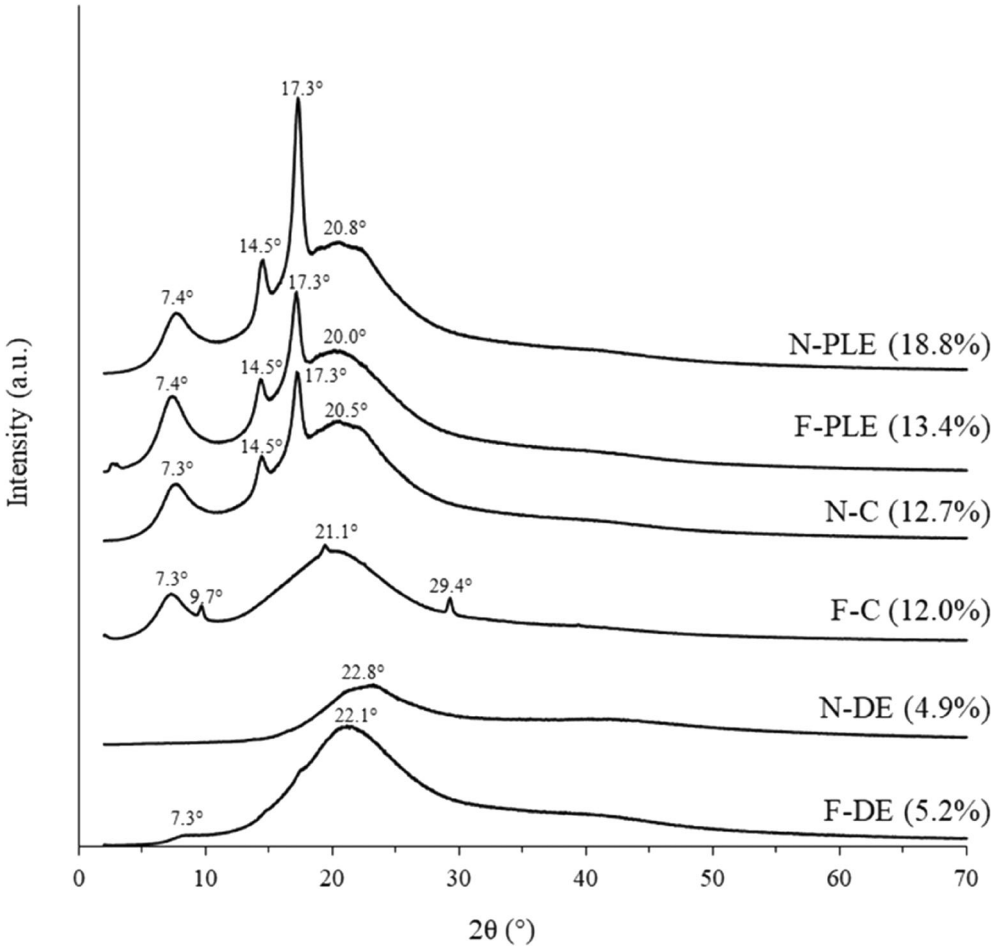

FIGURE 2 X-ray diffractograms of gelatin-based films (F) and nanocomposite films (N) control (C), with "Pitanga" leaf extract (PLE), or with double emulsion (DE). The values of crystallinity are presented over each spectrum.

These peaks confirm the semi-crystalline structure of gelatin.[26] The peaks at $2\theta = 14.5$ and 17.3°, present in F-PLE, N-C, and N-PLE, may be the result of some crystal formed by PLE and/or the crystalline structure of CN.[24]

In the N-DE, no peak relating to the α-helix structures was observed, while in the F-DE, only the peak at $2\theta = 7.3°$ was observed in low intensity. The formation of a protein complex between gelatin and sodium caseinate present in the external aqueous phase of DE, through hydrogen and ionic interactions, can reduce the formation of gelatin microcrystalline structures.[26] This may explain the disappearance of the characteristic peaks of the gelatin crystalline phase in the DE film and nanocomposite, and the fact that these treatments present the lowest crystallinity (Figure 2), as observed for sodium caseinate films incorporated with nanoemulsified cinnamon essential oil[26] and gelatin-based films reinforced with tannin-nanocellulose microgel.[1]

The crystallinity of films and nanocomposites ranged from 4.9 to 18.8%, in ascending order: N-DE < F-DE < F-C < N-C < F-PLE < N-PLE (Figure 2). N-PLE presented the highest crystallinity index, possibly due to the crystalline structures that NCs have and some crystals formed by PLE,[24,26] followed by F-PLE.

3.3 | Moisture content

The moisture content of all films and nanocomposites increased ($p < 0.05$) because of the conditioning RH increasing (Table 1), as could be expected, due to the hygroscopic character of gelatin and glycerol.[2] The same behavior was observed for cassava starch films containing glycerol or sorbitol[27] and gelatin/chitosan films containing glycerol.[28]

On another side, the moisture content of the films and nanocomposites was affected by the presence of CN, PLE, and/or DE, at the same RH (Table 1). Overall, F-PLE had the highest moisture content ($p < 0.05$) considering all RHs, while N-PLE had the lowest one ($p < 0.05$). The presence of CN and DE in the films and nanocomposites also generally reduced the moisture content, except at RH of 76%, where all treatments showed no difference ($p > 0.05$) in moisture content, except F-PLE, whose moisture content was the highest ($p < 0.05$).

The presence of PLE in F-PLE may have caused the higher moisture content in this film due to the hydrophilic groups of the PLE polyphenols. The greater number of hydrophilic groups in F-PLE, as well as

TABLE 1 Moisture content and thickness of gelatin-based films (F) and nanocomposite films (N) control (C), with "Pitanga" leaf extract (PLE), or with double emulsion (DE) at different relative humidity.

		Relative humidity (%)			
Properties	**Treatment**	**0**	**34**	**59**	**76**
Moisture content (%)	F-C	-	9.9 ± 0.7^{cA}	13.6 ± 0.2^{bB}	21.6 ± 1.1^{aAB}
	F-PLE	-	10.8 ± 0.4^{cA}	14.5 ± 0.2^{bA}	22.2 ± 0.4^{aA}
	F-DE	-	8.5 ± 0.4^{cB}	13.0 ± 0.1^{bBC}	19.6 ± 0.1^{aBC}
	N-C	-	8.7 ± 0.3^{cB}	13.3 ± 0.4^{bCD}	19.7 ± 0.4^{aBC}
	N-PLE	-	8.2 ± 0.1^{cB}	12.2 ± 0.4^{bCD}	19.4 ± 1.3^{aC}
	N-DE	-	8.2 ± 0.3^{cB}	12.0 ± 0.4^{bD}	20.0 ± 0.2^{aBC}
Thickness (μm)	F-C	69 ± 3^{dA}	83 ± 6^{cA}	100 ± 6^{bA}	119 ± 10^{aA}
	F-PLE	71 ± 3^{dA}	85 ± 4^{cA}	95 ± 4^{bA}	120 ± 5^{aA}
	F-DE	73 ± 5^{dA}	88 ± 7^{cA}	102 ± 10^{bA}	125 ± 12^{aA}
	N-C	70 ± 2^{dA}	86 ± 5^{cA}	98 ± 9^{bA}	129 ± 12^{aA}
	N-PLE	67 ± 3^{dA}	87 ± 3^{cA}	101 ± 7^{bA}	122 ± 6^{aA}
	N-DE	70 ± 4^{dA}	87 ± 2^{cA}	103 ± 5^{bA}	120 ± 8^{aA}

Note: Means ± standard deviation ($n = 3$). Different lowercase letters on the same line and different uppercase letters in the same column indicate significant differences between samples according to Tukey's test ($p < 0.05$).

interactions between gelatin and PLE, may increase sensitivity to water, as observed for gelatin-based films with haskap berries extract.[29] In the case of N-PLE, the observed effect was the opposite, since PLE polyphenols can interact with both CN and gelatin, forming a complex between PLE-CN-gelatin, which can reduce the free hydrophilic groups in this nanocomposite and, consequently, the moisture content.[25] The same trend was observed for gelatin and carboxymethylcellulose nanocomposites incorporated with pomegranate peel extract.[25]

Any decrease in moisture content due to treatments incorporated with CN and/or DE may be a consequence of the rigid structure of CN and the interactions of hydrogen with the hydrophilic groups of gelatin and the presence of oil in DE, which increases the hydrophobic character of the films and nanocomposites.[13,18] At RH of 76%, these influences were not evident, possibly because the higher moisture content can modify the interactions between the matrix components of the films and nanocomposites.

3.4 | Thickness

The mass of the film-forming solution deposited in the Petri dishes was controlled (1.25 g dry matter/Petri dish) and possibly for this reason no difference ($p > 0.05$) was observed in thickness between all treatments, at the same RH (Table 1). Regarding the effect of RH, as expected, the increase in RH caused an increase in the thickness of the films and nanocomposites due to the swelling of the material ($p < 0.05$).

Water absorption caused swelling in both materials,[10] with a linear increase in thickness (x) as a function of the moisture content (MC): $x = 2.3\text{MC} + 68.2$ ($R^2 = 0.915$) for films, and $x = 2.8\text{MC} + 67.0$ ($R^2 = 0.970$) for nanocomposites. Curiously, the presence of NC in the gelatin matrix slightly increased the swelling capacity of this material (2.8 μm/% of moisture) compared to films without NC (2.3 μm/% of moisture). Murray and Dutcher[30] also observed that chitosan films presented an increase in thickness as the conditioning RH increased, and the authors also attributed this behavior to the swelling phenomenon of the films due to water absorption.

3.5 | CO_2 and O_2 transmission rate

The gas permeation in biopolymeric films basically occurs in three stages: (i) the gas molecules adsorb on the biopolymeric surface (Henry's law); (ii) the dissolution/diffusion of gas molecules occurs through the biopolymer matrix, from the most concentrated area to the least concentrated (Fick's law); and (iii) finally, the desorption of gas molecules from the opposite surface of the biopolymer films occurs (Henry's law).[11]

The gas permeability of a biopolymer matrix therefore basically depends on the "solubility" of the gas in the films, which is affected by the chemical affinity between

TABLE 2 Oxygen transmission rate (O_2TR), carbon dioxide transmission rate (CO_2TR), and perm-selectivity ratio (CO_2/O_2) for gelatin-based films (F) and nanocomposite films (N) control (C), with "Pitanga" leaf extract (PLE), or with double emulsion (DE).

		Relative humidity (%)			
Parameter	**Treatment**	**0**	**34**	**59**	**76**
O_2TR (cm^3/m^2 d bar)	F-C	0.97 ± 0.01^{dE}	1.80 ± 0.00^{cE}	8.47 ± 0.05^{bC}	10.17 ± 0.15^{aC}
	F-PLE	2.90 ± 0.01^{dB}	3.26 ± 0.01^{cC}	12.70 ± 0.26^{aB}	9.77 ± 0.06^{bC}
	F-DE	5.67 ± 0.06^{cA}	1.27 ± 0.01^{dF}	15.20 ± 0.00^{bA}	28.83 ± 0.45^{aA}
	N-C	2.59 ± 0.01^{dC}	5.11 ± 0.07^{cA}	7.99 ± 0.27^{bC}	27.50 ± 0.36^{aB}
	N-PLE	2.88 ± 0.03^{bB}	2.49 ± 0.01^{cD}	3.22 ± 0.09^{aE}	1.53 ± 0.10^{dE}
	N-DE	2.47 ± 0.06^{dD}	4.83 ± 0.20^{cB}	5.97 ± 0.15^{bD}	6.50 ± 0.04^{aD}
CO_2TR (cm^3/m^2 d bar)	F-C	0.01 ± 0.00^{dF}	3.20 ± 0.20^{cD}	13.70 ± 0.26^{bA}	61.53 ± 3.09^{aB}
	F-PLE	2.82 ± 0.14^{dB}	3.74 ± 0.05^{cBC}	12.40 ± 0.26^{bB}	11.63 ± 0.21^{aE}
	F-DE	3.05 ± 0.10^{cA}	0.95 ± 0.01^{dE}	13.50 ± 0.10^{bA}	21.20 ± 0.17^{aD}
	N-C	1.93 ± 0.02^{dD}	3.43 ± 0.23^{cCD}	4.65 ± 0.01^{bE}	40.40 ± 0.20^{aC}
	N-PLE	1.43 ± 0.06^{dE}	4.87 ± 0.07^{cA}	6.20 ± 0.04^{bD}	148.33 ± 5.18^{aA}
	N-DE	2.27 ± 0.09^{dC}	3.91 ± 0.07^{cB}	7.80 ± 0.41^{bC}	6.02 ± 0.18^{aE}
CO_2/O_2	F-C	0.01 ± 0.00^{cD}	1.78 ± 0.11^{bB}	1.62 ± 0.03^{bB}	6.05 ± 0.52^{aB}
	F-PLE	0.97 ± 0.05^{bA}	1.15 ± 0.01^{aC}	0.98 ± 0.00^{bD}	1.19 ± 0.03^{aC}
	F-DE	0.54 ± 0.01^{cC}	0.75 ± 0.01^{bD}	0.89 ± 0.01^{aD}	0.89 ± 0.02^{aC}
	N-C	074 ± 0.01^{bB}	0.67 ± 0.05^{bD}	0.58 ± 0.02^{aE}	1.47 ± 0.02^{aC}
	N-PLE	0.50 ± 0.02^{cC}	1.96 ± 0.03^{bA}	1.93 ± 0.05^{bA}	30.09 ± 2.65^{aA}
	N-DE	0.92 ± 0.03^{bA}	0.81 ± 0.03^{cD}	1.31 ± 0.08^{aC}	0.93 ± 0.02^{bC}

Note: Means ± standard deviation ($n = 3$). Different lowercase letters on the same line and different uppercase letters in the same column indicate significant differences between means, according to Tukey's test ($p < 0.05$).

the gas molecules and film components influenced by polarity, molecular weight, and size, and by those conditions that affect the gas diffusivity, such as film crystallinity, porosity, thickness, homogeneity, among others.[11] Evidently, external conditions, such as pressure difference, temperature and RH can also influence gas permeability. Generally, biopolymers-based films have good gas barrier properties at low RH,[31] but still perform worse than synthetic plastics.

The films gas transmission rate (GTR) of O_2 (O_2TR) and CO_2 (CO_2TR) presented different behaviors and trends as a function of RH and treatment (Table 2). This behavior occurred because, as observed in the SEM images (Figure 1) and X-ray patterns (Figure 2), the structure of the films and nanocomposites was affected by the film composition (with PLE or DE, with or without CN). Therefore, different treatments were expected to show different gas permeability behaviors of the films.

Regarding the effect of RH, the O_2TR and CO_2TR increased, in general, with increasing RH, except for F-DE, where both GTR decreased at RH of 34% and then increased at other RH levels. For N-PLE, the O_2TR decreased at RH of 76%, and for N-DE, the CO_2TR decreased at RH of 76%. As previously noted, increasing RH leads to an increase in the moisture content of films and nanocomposites, causing a plasticizing effect.[2]

Plasticization of films and nanocomposites results in an increase in macromolecular free volume or, in other words, an increase in macromolecular mobility, facilitating gases permeation into the biopolymer matrix.[10,11] Although GTR is influenced by film thickness, it is expected to be independent of it for thicker samples (>10 μm).[32] Kurek et al.[31] also observed that carvacrol-activated chitosan films and coatings presented increased O_2TR and CO_2TR with increased RH. The same behavior was observed for films based on whey protein isolate.[33]

The effect of films and nanocomposites composition was also observed. Under dry conditions (RH = 0%), F-C, which does not contain PLE, DE, or CN, presented the lowest values of O_2TR and CO_2TR, and it was practically impermeable to CO_2 (CO_2TR ~0.01 cm^3/m^2 d bar). Also, for the other treatments, O_2TR was higher than CO_2TR, varying from 2.5 to 5.7 (cm^3/m^2 d bar) and from 1.4 to 3.1 (cm^3/m^2 d bar), respectively, with F-DE presenting the highest values for both gases. This may have occurred because the oil present in DE can create microchannels

or porosity in the structure of the films, facilitating gas permeation under these conditions. The effect of DE was less pronounced in N-DE, possibly because of chemical interactions that occurred between gelatin-DE-CN, forming a more cohesive matrix that was difficult to penetrate.

The fact that CO_2TR was lower than O_2TR in all treatments at RH = 0% can be explained by the fact that the size of the CO_2 molecule is larger than that of O_2 (3.4 and 3.1 Å, respectively),[34] which makes passage through the dehydrated biopolymeric matrix difficult (Figure 1). The same behavior was observed for chitosan-coated polyethylene films by Kurek et al.[31]

In the other RHs, the effects observed were varied, because of the presence of water in the biopolymer matrix. F-C, F-PLE, and N-PLE presented higher CO_2TR than O_2TR at RHs of 34%, 59%, and 76%, possibly related to the fact that CO_2 has a higher solubility in water than O_2, thus increasing the permeation of this gas in the hydrated material.[35] This greater solubility of CO_2 in water can also be explained by the fact that it can react with water to form carbonic acid. Furthermore, CO_2 can interact with the free amino groups of gelatin, increasing its sorption and permeation, unlike O_2.[36] Kurek et al.[31] observed that, in hydrated chitosan-based films and coatings, the CO_2TR was higher than the O_2TR, and attributed this behavior to the greater solubility of CO_2 in water.

Under these same conditions, O_2TR was greater than CO_2TR in F-DE, N-C, and N-DE. For F-DE and N-DE, this behavior can be explained by the presence of DE oil, which can increase the non-polar character of these materials, causing non-polar molecules such as O_2 and CO_2 to have greater affinity. In these cases, the O_2 molecule, being smaller, was probably able to migrate more easily through the biopolymeric matrix.[35] The presence of oil can also affect all chemical interactions and rearrangements in biopolymer matrices, influencing the affinity of CO_2 for the amino groups of gelatin and for water. In particular, F-DE presented the lowest values of O_2TR and CO_2TR at RH = 34%, possibly because, in this condition, the chemical interactions (such as hydrogen interaction) between gelatin and sodium caseinate present in the external aqueous phase of DE, in the presence of water, have been maximized, forming a more compact structure. In the remaining RH (59 and 76%), O_2TR and CO_2TR were, in general, among the highest in F-DE, given that increasing the amount of water present in the film can rehydrate the gelatin, causing destabilization and separation of the DE oil. This separation can compromise the film structure and form pores, which can create a preferential path for gas permeation.

N-PLE presented the lowest O_2TR values ($p < 0.05$) at RH = 59 and 76%. This could be a consequence of its greater crystallinity (Figure 2) since the permeation of gases and vapors occurs in the amorphous portion.[34] Overall, crystallinity plays a fundamental role as gases cannot diffuse and permeate through the crystalline phase due to the restricted mobility of the biopolymer chain.[10] Biopolymer matrix crystals are impenetrable to gas molecules and consequently biopolymers with the highest crystallinity were generally the best barrier materials. N-C, on the other hand, presented a lower crystallinity index than N-PLE; therefore, higher O_2TR and CO_2TR values. Although N-DE had a lower crystallinity index, its O_2TR was the lowest at RH = 76%, possibly because of the gelatin-DE-CN interaction.

Overall, the O_2TR and CO_2TR values of the films and nanocomposites were lower than the values reported for modified polylactic acid-based films at 23°C and 26% RH (4–487 and 5–1200 cm^3/m^2 d bar, respectively).[37] The O_2TR and CO_2TR values were also lower than those of common polymer-based packaging at 23°C and 0 or 50% RH, such as polypropylene (50–100 and 270–1000 cm^3/m^2 d bar, respectively), polyethylene (50–200 and 200–900 cm^3/m^2 d bar, respectively) and polystyrene (100–150 and 270–1000 cm^3/m^2 d bar, respectively); however, they were higher than those of high barrier performance packaging, such as polyamide (0.1–1 and 1.8–4.6 cm^3/m^2 d bar, respectively), polyvinyl alcohol (0.02 and 0.04 cm^3/m^2 d bar, respectively), and ethylene vinyl alcohol (0.001–0.01 and 0.01–0.08 cm^3/m^2 d bar, respectively).[38,39] These comparisons should be made cautiously, as many conditioning and analysis conditions are used in the literature. However, they can be useful for positioning the films and nanocomposites from this study relative to the state of the art.

The gas permeability ratio (CO_2TR/O_2TR, also called perm-selectivity ratio) is also an important parameter for food packaging, as it informs about the proportion of gases inside the packaging[40] and about what type of food it is suitable for. The CO_2TR/O_2TR perm-selectivity ratio is already known for several polymers. According to Schmid et al.,[33] for non-condensable gases, the gas perm-selectivity ratio is relatively constant and is not related to the polymer chemical structure. This means that although the molecular size of permeating species could affect the transmission rate, in the case of O_2 and CO_2 there is no relationship between gas molecular size and permeability behavior.[34] Generally, in biopolymeric films, CO_2 is much more permeable than O_2, as it has a higher solubility in water and a higher affinity for gelatin, for example, as previously mentioned.[36] Therefore, the CO_2TR/O_2TR value in gelatin-based films is generally greater than 1.

In this study, O_2TR was higher than CO_2TR for all treatments at RH = 0%, and the CO_2TR/O_2TR ranged

from 0.01 to 0.97 (Table 2). In the other RHs, F-DE and N-DE presented higher O_2TR than CO_2TR, with CO_2TR/O_2TR smaller than 1, except for N-DE in RH = 59% (CO_2TR/O_2TR = 1.31). In the other treatments, the CO_2TR/O_2TR was greater than 1, with values varying between 1.15 and 1.96, except for F-C at RH = 76%, where the value was 6.05. This result indicates that, in films and nanocomposites with some incorporated component (CN, PLE, and/or DE), the CO_2 permeability was reduced and the CO_2TR/O_2TR ratio remained practically constant, possibly because the hydrogen interactions occurring between gelatin and these components reduced the free amino groups in gelatin, for which the CO_2 molecule has affinity. The CO_2TR/O_2TR ratio values determined for the films and nanocomposites may be interesting for packaging foods with a high respiration rate, such as fruits and vegetables, since values <3 have been considered as ideal for optimizing the respiration rate of these fresh foods.[41,42]

In summary, all studied films and nanocomposites can be considered as medium barrier to O_2 (400–4000 cm^3 µm/m^2 d bar[32]), with the best performances being observed at RH = 0% and 34%. Especially, N-PLE and N-DE presented good O_2 barrier properties at higher RH (59 and 76%). The main novelty of this study was to obtain films and nanocomposites based on biopolymers with average barrier performance to O_2 and CO_2 gases, higher than that of packaging based on polymers, such as polyethylene and polystyrene. This performance was obtained by combining the effect of adding a plant extract rich in phenolic compounds encapsulated in double emulsions and cellulose nanocrystals, which performed interactions with the biopolymer matrix. In addition, these materials, especially the nanocomposites, were able to maintain the ratio between CO_2TR and O_2TR, despite the increase in relative humidity.

4 | CONCLUSIONS

The O_2 and CO_2 permeability of gelatin-based films and nanocomposites activated with non-encapsulated PLE and encapsulated in double emulsion was influenced mainly by the rearrangement of chemical interactions occurring in the biopolymeric matrix because of their moisture content. The increase in relative humidity provoked an increase in the moisture content of these materials, thus contributing to the occurrence of phenomena such as swelling, the increase in free volume in the biopolymer matrix due to the water plasticizing effect and, consequently, the increase in gas permeability. At higher relative humidity, the nanocomposites generally presented the best gas barrier properties, especially the nanocomposite with double emulsion, for both gases, and the non-encapsulated PLE nanocomposite, with lower O_2 permeability. Accordingly, the addition of crystalline nanocellulose and non-encapsulated or doubly emulsified PLE into gelatin-based films improved the gas barrier properties, especially under high relative humidity conditions.

AUTHOR CONTRIBUTIONS

Larissa Tessaro: Conceptualization (equal); data curation (equal); formal analysis (equal); investigation (equal); methodology (equal); validation (equal); visualization (equal); writing – original draft (equal). **Paula Benoso**: Data curation (equal); formal analysis (equal); investigation (equal); methodology (equal); writing – original draft (supporting). **Valentina Siracusa**: Data curation (equal); formal analysis (equal); methodology (equal); supervision (equal); writing – review & editing (supporting). **Rodrigo Vinícius Lourenço**: Data curation (equal); formal analysis (equal); methodology (equal); validation (equal). **Marco Dalla Rosa**: Methodology (equal); resources (equal); supervision (equal); visualization (equal); writing – review & editing (supporting). **Paulo José do Amaral Sobral**: Conceptualization (lead); formal analysis (equal); funding acquisition (lead); methodology (equal); project administration (lead); resources (lead); supervision (lead); writing – review & editing (lead).

ACKNOWLEDGMENTS

The authors acknowledge the São Paulo Research Foundation (FAPESP) for the grants (2013/07914-8) and the Brazilian National Council for Scientific and Technological Development (CNPq), for the Grant (40.3746/2021-3) and Research fellowship of P.J.A.S. (30.2482/2022-9). This study was financed in part by the "Coordenação de Aperfeiçoamento de Pessoal de Nível Superior-Brasil" (CAPES)-PhD fellowship of L.T. (Finance Code 001) L. T. and PhD split fellowship of P.B. (88887.716839/2022-00). The Article Processing Charge for the publication of this research was funded by the Coordenação de Aperfeiçoamento de Pessoal de Nível Superior - Brasil (CAPES) (ROR identifier: 00x0ma614).

CONFLICT OF INTEREST STATEMENT

The authors declare no conflicts of interest.

DATA AVAILABILITY STATEMENT

The datasets generated and/or analyzed during the current study are available from the corresponding author on reasonable request.

ORCID

Larissa Tessaro https://orcid.org/0000-0002-1670-9802
Valentina Siracusa https://orcid.org/0000-0001-9055-

5082

Marco Dalla Rosa https://orcid.org/0000-0002-0405-7026

Paulo José do Amaral Sobral https://orcid.org/0000-0002-3913-3172

REFERENCES

1. Li M, Guo L, Mu Y, et al. Gelatin films reinforced by tannin-nanocellulose microgel with improved mechanical and barrier properties for sustainable active food packaging. *Food Hydrocoll*. 2024;149:109642. doi:10.1016/j.foodhyd.2023.109642
2. Sobral PJA, Menegalli FC, Hubinger MD, Roques MA. Mechanical, water vapor barrier and thermal properties of gelatin based edible films. *Food Hydrocoll*. 2001;15:423-432. doi:10.1016/S0268-005X(01)00061-3
3. Sobral PJA, Habitante AMQB. Phase transitions of pigskin gelatin. *Food Hydrocoll*. 2001;15:377-382. doi:10.1016/S0268-005X(01)00060-1
4. Hanani ZAN, Roos YH, Kerry JP. Use and application of gelatin as potential biodegradable packaging materials for food products. *Int J Biol Macromol*. 2014;71:94-102. doi:10.1016/j.ijbiomac.2014.04.027
5. Acharya DR, Liu S, Lu H, et al. Nanoemulsion-integrated gelatin/bacterial cellulose nanofibril-based multifunctional film: fabrication, characterization, and application. *Int J Biol Macromol*. 2024;257:128341. doi:10.1016/j.ijbiomac.2023.128341
6. Al-Maqtari QA, Al-Gheethi AAS, Ghaleb AD, et al. Fabrication and characterization of chitosan/gelatin films loaded with microcapsules of *Pulicaria jaubertii* extract. *Food Hydrocoll*. 2022;129:107624. doi:10.1016/j.foodhyd.2022.107624
7. Bonilla J, Sobral PJA. Antioxidant and physicochemical properties of blended films based on gelatin-sodium caseinate activated with natural extracts. *J Appl Polym Sci*. 2017;134:44467. doi:10.1002/app.44467
8. Flaker CHC, Lourenço RV, Bittante AMQB, Sobral PJA. Gelatin-based nanocomposite films: a study on montmorillonite dispersion methods and concentration. *J Food Eng*. 2015;167:65-70. doi:10.1016/j.jfoodeng.2014.11.009
9. Ilyas RA, Azmi A, Nurazzi NM, et al. Oxygen permeability properties of nanocellulose reinforced biopolymer nanocomposites. *Mater Today Proc*. 2022;52:2414-2419. doi:10.1016/j.matpr.2021.10.420
10. Xue W, Zhu J, Sun P, Yang F, Wu H, Li W. Permeability of biodegradable film comprising biopolymers derived from marine origin for food packaging application: a review. *Trends Food Sci Technol*. 2023;136:295-307. doi:10.1016/j.tifs.2023.05.001
11. Trinh BM, Chang BP, Mekonnen TH. The barrier properties of sustainable multiphase and multicomponent packaging materials: a review. *Prog Mater Sci*. 2023;133:101071. doi:10.1016/j.pmatsci.2023.101071
12. Martelli-Tosi M, Masson MM, Silva NC, et al. Soybean straw nanocellulose produced by enzymatic or acid treatment as a reinforcing filler in soy protein isolate films. *Carbohydr Polym*. 2018;198:61-68. doi:10.1016/j.carbpol.2018.06.053
13. Tessaro L, Lourenço RV, Martelli-Tosi M, Sobral PJA. Gelatin/chitosan based films loaded with nanocellulose from soybean straw and activated with "Pitanga" (*Eugenia uniflora* L.) leaf hydroethanolic extract in W/O/W emulsion. *Int J Biol Macromol*. 2021;186:328-340. doi:10.1016/j.ijbiomac.2021.07.039
14. Fukuzumi H, Saito T, Iwata T, Kumamoto Y, Isogai A. Transparent and high gas barrier films of cellulose nanofibers prepared by TEMPO-mediated oxidation. *Biomacromolecules*. 2009;10:162-165. doi:10.1021/bm801065u
15. Luciano CG, Tessaro L, Lourenço RV, Bittante AMQB, Fernandes AM, Sobral PJA. Bi-layer gelatin active films with "Pitanga" leaf hydroethanolic extract and/or natamycin in the second layer. *J Appl Polym Sci*. 2021;138:51246. doi:10.1002/app.51246
16. Luciano CG, Tessaro L, Bonilla J, Balieiro JC d C, Trindade MA, Sobral PJA. Application of bi-layers active gelatin films for sliced dried-cured Coppa conservation. *Meat Sci*. 2022;189:108821. doi:10.1016/j.meatsci.2022.108821
17. Lorenzo JM, Vargas FC, Strozzi I, et al. Influence of pitanga leaf extracts on lipid and protein oxidation of pork burger during shelf-life. *Food Res Int*. 2018;114:47-54. doi:10.1016/j.foodres.2018.07.046
18. Tessaro L, Luciano CG, Bittante AMQB, Lourenço RV, Martelli-Tosi M, Sobral PJA. Gelatin and/or chitosan-based films activated with "Pitanga" (*Eugenia uniflora* L.) leaf hydroethanolic extract encapsulated in double emulsion. *Food Hydrocoll*. 2021;113:106523. doi:10.1016/j.foodhyd.2020.106523
19. Tessaro L, Martelli-Tosi M, Sobral PJA. Development of W/O emulsion for encapsulation of "Pitanga" (*Eugenia uniflora* L.) leaf hydroethanolic extract: droplet size, physical stability and rheology. *Food Sci Technol*. 2022;42:1-8. doi:10.1590/fst.65320
20. Tessaro L, Luciano CG, Martins MFL, Ramos AP, Martelli-Tosi M, Sobral PJA. Stable and bioactive W/O/W emulsion loaded with "Pitanga" (*Eugenia uniflora* L.) leaf hydroethanolic extract. *J Dispers Sci Technol*. 2022;43:1890-1900. doi:10.1080/01932691.2021.1949339
21. Gontard N, Guilbert S, Cuq J-L. Edible wheat gluten films: influence of the main process variables on film properties using response surface methodology. *J Food Sci*. 1992;57:190-195. doi:10.1111/j.1365-2621.1992.tb05453.x
22. Siracusa V, Karpova S, Olkhov A, Zhulkina A, Kosenko R, Iordanskii A. Gas transport phenomena and polymer dynamics in PHB/PLA blend films as potential packaging materials. *Polymers*. 2020;12:647. doi:10.3390/polym12030647
23. Siracusa V, Ingrao C. Correlation amongst gas barrier behaviour, temperature and thickness in BOPP films for food packaging usage: a lab-scale testing experience. *Polym Test*. 2017;59:277-289. doi:10.1016/j.polymertesting.2017.02.011
24. Luciano CG, Rodrigues MM, Lourenço RV, Bittante AMQB, Fernandes AM, Sobral PJA. Bi-layer gelatin film: activating film by incorporation of "Pitanga" leaf hydroethanolic extract and/or Nisin in the second layer. *Food Bioproc Tech*. 2021;14:106-119. doi:10.1007/s11947-020-02568-w
25. Vargas-Torrico MF, Aguilar-Méndez MA, Ronquillo-de Jesús E, Jaime-Fonseca MR, von Borries-Medrano E. Preparation and characterization of gelatin-carboxymethylcellulose active film incorporated with pomegranate (*Punica granatum* L.) peel extract for the preservation of raspberry fruit. *Food Hydrocoll*. 2024;150:109677. doi:10.1016/j.foodhyd.2023.109677
26. Ranjbaryan S, Pourfathi B, Almasi H. Reinforcing and release controlling effect of cellulose nanofiber in sodium caseinate

films activated by nanoemulsified cinnamon essential oil. *Food Packag Shelf Life*. 2019;21:100341. doi:10.1016/j.fpsl.2019.100341

27. Lagos JB, Vicentini NM, dos Santos RMC, Bittante AMQB, Sobral PJA. Mechanical properties of cassava starch films as affected by different plasticizers and different relative humidity conditions. *Int J Food Sci*. 2015;4:116-125. doi:10.7455/ijfs/4.1.2015.a10
28. Benbettaïeb N, Debeaufort F, Karbowiak T. Bioactive edible films for food applications: mechanisms of antimicrobial and antioxidant activity. *Crit Rev Food Sci Nutr*. 2019;59:3431-3455. doi:10.1080/10408398.2018.1494132
29. Liu J, Yong H, Liu Y, Qin Y, Kan J, Liu J. Preparation and characterization of active and intelligent films based on fish gelatin and haskap berries (*Lonicera caerulea* L.) extract. *Food Packag Shelf Life*. 2019;22:100417. doi:10.1016/j.fpsl.2019.100417
30. Murray CA, Dutcher JR. Effect of changes in relative humidity and temperature on ultrathin chitosan films. *Biomacromolecules*. 2006;7:3460-3465. doi:10.1021/bm060416q
31. Kurek M, Guinault A, Voilley A, Galić K, Debeaufort F. Effect of relative humidity on carvacrol release and permeation properties of chitosan based films and coatings. *Food Chem*. 2014;144:9-17. doi:10.1016/j.foodchem.2012.11.132
32. Wang J, Gardner DJ, Stark NM, Bousfield DW, Tajvidi M, Cai Z. Moisture and oxygen barrier properties of cellulose nanomaterial-based films. *ACS Sustain Chem Eng*. 2018;6:49-70. doi:10.1021/acssuschemeng.7b03523
33. Schmid M, Zillinger W, Müller K, Sängerlaub S. Permeation of water vapour, nitrogen, oxygen and carbon dioxide through whey protein isolate based films and coatings—Permselectivity and activation energy. *Food Packag Shelf Life*. 2015;6:21-29. doi:10.1016/j.fpsl.2015.08.002
34. Gigli M, Lotti N, Gazzano M, et al. Biodegradable aliphatic copolyesters containing PEG-like sequences for sustainable food packaging applications. *Polym Degrad Stab*. 2014;105:96-106. doi:10.1016/j.polymdegradstab.2014.04.006
35. Galus S, Kadzińska J. Food applications of emulsion-based edible films and coatings. *Trends Food Sci Technol*. 2015;45:273-283. doi:10.1016/j.tifs.2015.07.011
36. Biscarat J, Charmette C, Sanchez J, Pochat-Bohatier C. Development of a new family of food packaging bioplastics from cross-linked gelatin based films. *Can J Chem Eng*. 2015;93:176-182. doi:10.1002/cjce.22077
37. Siracusa V, Blanco I, Romani S, Tylewicz U, Rocculi P, Rosa MD. Poly(lactic acid)-modified films for food packaging application: physical, mechanical, and barrier behavior. *J Appl Polym Sci*. 2012;125:E390-E401. doi:10.1002/app.36829
38. Lange J, Wyser Y. Recent innovations in barrier technologies for plastic packaging—a review. *Packag Tech Sci*. 2003;16:149-158. doi:10.1002/PTS.621
39. Vandewijngaarden J, Murariu M, Dubois P, et al. Gas permeability properties of poly(3-hydroxybutyrate-co-3-hydroxyhexanoate). *J Polym Environ*. 2014;22:501-507. doi:10.1007/s10924-014-0688-1
40. Barbato A, Apicella A, Malvano F, Scarfato P, Incarnato L. High-barrier, biodegradable films with polyvinyl alcohol/polylactic acid + wax double coatings: influence of relative humidity on transport properties and suitability for modified atmosphere packaging applications. *Polymers*. 2023;15:4002. doi:10.3390/polym15194002
41. Mangaraj S, Goswami TK, Mahajan PV. Applications of plastic films for modified atmosphere packaging of fruits and vegetables: a review. *Food Eng Rev*. 2009;2:133-158. doi:10.1007/s12393-009-9007-3
42. Al-Ati T, Hotchkiss JH. The role of packaging film Permselectivity in modified atmosphere packaging. *J Agric Food Chem*. 2003;51:4133-4138. doi:10.1021/jf034191b

How to cite this article: Tessaro L, Benoso P, Siracusa V, Lourenço RV, Dalla Rosa M, Sobral PJdA. The conditioning relative humidity influences the gas permeability of active films and nanocomposites based on gelatin. *Polym Eng Sci*. 2025;1-12. doi:10.1002/pen.27235